Highlights of Spanish Astrophysics VIII, Proceedings of the XI Scientific Meeting of the Spanish Astronomical Society held on September 8–12, 2014, in Teruel, Spain. A. J. Cenarro, F. Figueras, C. Hernández-Monteagudo, J. Trujillo Bueno, and L. Valdivielso (eds.)

IRIS observations and 3D 'realistic' MHD models of the solar chromosphere

Viggo Hansteen[1], Mats Carlsson[1], and Boris Gudiksen[1]

[1] Institute of Theoretical Astrophysics, University of Oslo, PB 1029 Blindern, 0315 Oslo Norway

Abstract

The Interface Region Imaging Spectrograph (IRIS) is a NASA "Small Explorer" mission. It was launched in late June 2013 and since then it has obtained spectra and images from the outer solar atmosphere at unprecedented spatial and temporal resolution. Its primary goal is to probe the photosphere-corona interface: the source region of outer atmosphere heating and dynamics and a region that has an extremely complicated interplay between plasma, radiation and magnetic field. The scientific justification for IRIS hinges on the capabilities of 3D magnetohydrodynamic models to allow the confident interpretation of observed data. The interplay between observations and modeling is discussed, illustrated with examples from recent IRIS observations.

1 Introduction

Launched in June 2013, the Interface Region Imaging Spectrograph (IRIS) satellite allows the observation of simultaneous spectra and images of the photosphere, mid to upper chromosphere, transition region, and corona with better than 0.4 arcsec spatial resolution, at high cadence and good spectral resolution [6]. IRIS is specifically designed to study the transport of energy and mass through the solar chromosphere and transition region into the corona, thus shedding light on one of the great unsolved problems of solar physics. An example of IRIS observables are shown in Figure 1. Typically, IRIS builds up images by rastering the slit across the region of interest. Both chromospheric and transition region observables are formed in a very complex magnetohydrodynamic environment and are in part optically thick; thus, extensive numerical analysis is required before observations can be translated into the physical parameters that describe the system. This can be done either by inversions or by forward modelling, where synthetic spectral lines are computed on the basis of 'realistic' 3D magnetohydrodynamic models and are compared directly to the observations themselves.

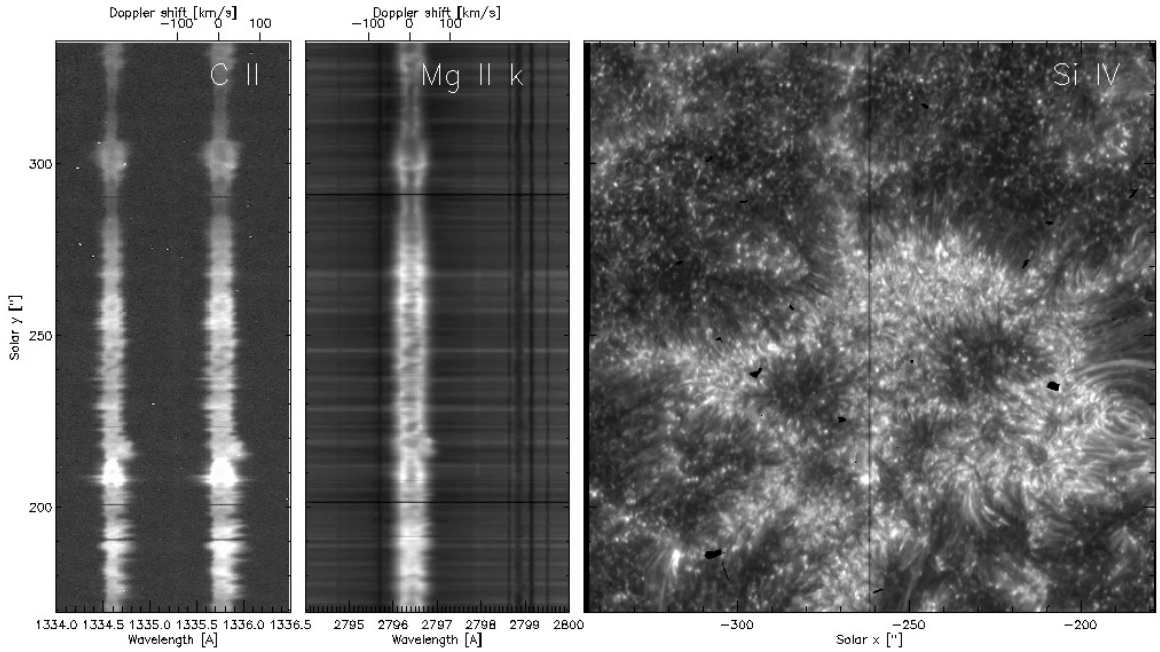

Figure 1: Example of the IRIS data products showing the sprectral lines of the upper chromosphere/lower transition region C II lines and the Mg II k line formed in the mid to upper chromosphere. In the right panel a slit jaw image in the Si IV band centered near 140.0 nm is shown.

From the very outset the IRIS project included such numerical simulations as an integral part of the mission.

Solar activity and the heating of the outer solar atmosphere has as its root cause the interaction between convective motions and the solar magnetic field in the solar photosphere and below. Though the basic elements of this process have been clear for several decades [e.g. 1], the complexity of the atmosphere has precluded consensus on the detailed mechanisms and their relative importance. In the solar photosphere we find a high β plasma (the ratio of the gas pressure to the magnetic pressure $p_{\rm g}/p_{\rm B}$) in continual motion; the top of the Sun's convective envelope in which the magnetic field is embedded, in structures varying in size from sub granular (< 1000 km) to large spots (up to several 10 000 km). At temperatures of $< 10\,000$ K the pressure scale height is only a few hundred kilometers while the magnetic field is organized such that its scale height is roughly an order of magnitude larger. Thus, already only 1000 km above the solar surface, and even in regions of relatively weak magnetic fields (so called "quiet Sun" regions) we find that plasma β drops below one and that the magnetic field controls the dynamics and energetics in the overlying chromosphere and corona.

Observations show that magnetic flux continually erupts or emerges everywhere on the solar surface, is churned by granular motions, and is recycled rapidly. We find mixed polarity regions on granular (1000 km) and super-granular (10 000 km) scales in the quiet Sun, while

the field appears more unipolar (on these scales) in "active Sun", plage and sunspot regions. The emergence and displacement of magnetic flux at photospheric heights as the plasma does work on the field imply an vertically propagating Poynting flux; the dissipation of this flux in the outer atmosphere is called "AC" or wave heating when the timescales or periods of field motions is short and "DC" heating when the timescale of motions is much longer than the typical wave propagation time along a magnetic field line. There is a rich literature discussing both forms of heating [e.g. 18, 15].

In this paper we will describe the state of the art of numerical modelling of the outer solar atmosphere and compare its results with observations of the mid to upper chromosphere and transition region, in particular concentrating on observations taken with the IRIS satellite. Some of the text below also appears in the proceedings of the ASTRONUM 2014 conference in which a similar lecture was given by the first author of this manuscript.

2 Magnetic braiding and nanoflare heating of the corona

Parker [21] conceived the corona as composed of the set of field lines joining two separated regions of the photosphere in which the magnetic field is anchored. He then remarked that coronal heating could proceed as a result of the dissipation of the many small current sheets that form as a consequence of continuous field line shuffling and intermixing in the photosphere. He proposed that the dissipation would proceed in a large number of localized impulsive bursts of energy that he termed "nanoflares" with an average energy of some 10^{17} J.

The work of Parker has been put on a firmer footing by numerical "braiding" experiments [14, 7] in which the original schematic "Parker corona" consisting of two photospheric plates joined by anchored, initially straight, magnetic field lines spanning the corona is inserted in a computational box. The system is subjected to random large scale shearing motions on the two boundaries and the resistive MHD equations are used to follow the evolution of the field. They find that indeed such motions lead to the formation of current sheets where both the current and Joule dissipation in the computational box initially grow exponentially, reaching a statistically steady state after a few correlation times. The heating rate depends on the boundary velocity amplitude and correlation time, Alfvén speed, and initial magnetic field strength, but is to first order independent of resistivity.

The numerical work of Galsgaard & Nordlund was extended in Gudiksen & Nordlund [9] in which the schematic "straight" corona was replaced by a much more realistic computational box including gravity, a simple chromosphere, field lines having curvature, and field aligned conductive flux. The initial magnetic field was calculated on the basis of an observed magnetogram of an active region using a potential field extrapolation. The field was line tied to the photosphere and stressed using the constructed granulation pattern and its amplitude and vorticity power spectra. This boundary condition generated a Poynting flux that led to a dissipated energy in the modeled corona of $[3-4] \times 10^{\ 3}$ W/m^2, sufficient to maintain an average temperature of 1 MK and for which simulated images of EUV emission reproduced observed photon count rates.

3 Numerical challenges in modelling the outer solar atmosphere

Earlier work described in the previous section show that the braiding mechanism is a viable process in producing the Solar corona, though the question remains whether the many assumptions that went into these earlier simulations are critical to this conclusion. In particular, the role of the chromosphere which fills some 10-20 pressure scale heights between the photosphere and corona and which goes from gas dominated ($\beta > 1$) to field dominated ($\beta < 1$) was largely ignored.

The Bifrost code [8] was designed to model the solar atmosphere from the (upper) convection zone to corona. The goal of this work was to construct models with enough realism that meaningful comparisons between synthesized and observed spectra could be made, *i.e.* to go beyond confirming that enough energy is being dissipated in the upper solar atmosphere towards making assessments of the relative role of various detailed heating mechanisms.

In addition to a well functioning MHD code the following elements are necessary ingredients in constructing a numerical model of sufficient realism to compare directly with observations: Radiative transfer in the photosphere and lower chromosphere. A realistic equation of state. A description of the radiative losses in the middle to upper chromosphere, transition region and corona that is fast while correctly representing the energetics of the upper atmosphere. And finally, a method for treating conductive flux along the magnetic field.

Numerical simulations of solar and stellar surface convection has been carried out for several decades [see 20] and have passed a number of "reality checks" by comparisons with observational data [22] as well as "code vs. code" comparisons [2]. In short, it seems that the solar granulation pattern, implying the velocity and temperature structure near the photosphere as well, is well reproduced in these models. In the Bifrost code described here radiative transfer is implemented with coherent scattering [24], using a short-characteristics based method to compute the radiative flux divergence for the energy equation [13].

At greater heights the radiative energy balance in the solar chromosphere is dominated by strong spectral lines that are formed very far from LTE. It is computationally prohibitive to solve the full equations of radiative transfer for these lines. Instead, based on detailed calculations, simple recipes have been derived that allow the use of empirical formula for radiative heating and cooling [3].

As the temperature approaches 1 MK and beyond thermal conduction becomes one of the major terms in the energy equation. Since thermal conduction is described by a second order diffusion operator, the inclusion of it into an explicit MHD code causes certain difficulties: the CFL-condition for a diffusive operator scales as $\Delta x^{\,2}$ rather than Δx for the other magnetohydrodynamic operators. This severely limits the time step Δt the code can be stably run at. In the Bifrost code this problem is solved by operator splitting and thereafter solving the conductive operator implicitly using a multi-grid solver [8].

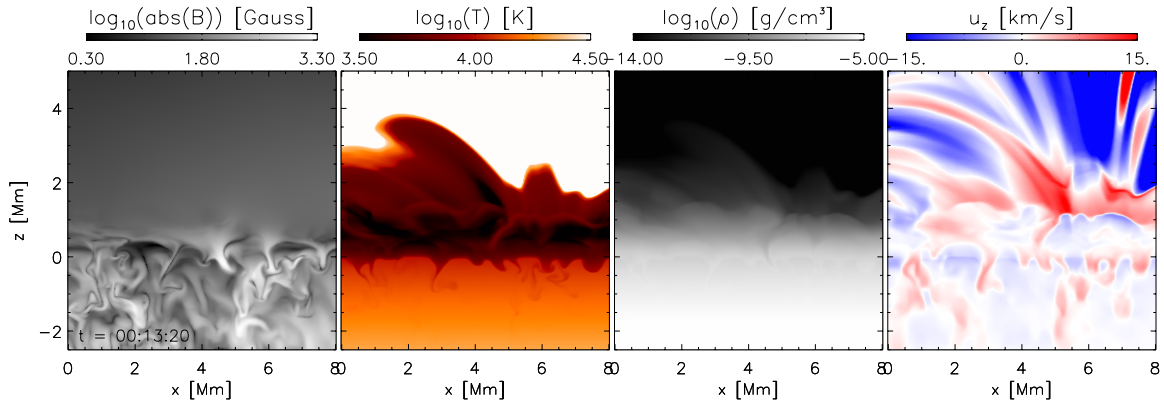

Figure 2: Vertical slice through a Bifrost model chromosphere. From left to right we find the magnitude of magnetic field $|B|$, the temperature, the density ρ, and the vertical velocity u_z in a cutout of a model of size $24 \times 24 \times 17$ Mm.

4 Results and comparisons with observations

Once the gravity, effective temperature and chemical composition of the plasma is set there are in reality no other free parameters that determine the evolution of hydrodynamical surface convection simulations. The case becomes very different when the magnetic field is included: the solar photosphere displays a wide variety of magnetic field strengths and distributions on the surface from magnetic elements at or below current observational limits (say 70 km) to sunspot groups (active regions) of more than 100 Mm. In addition, the weak small scale field is not well constrained observationally, even though much progress has been made in the last decade since the launch of Hinode and SDO.

In figure 2 we show a typical slice through the Bifrost modeled chromosphere. In the Bifrost modeled chromosphere we find that for a large span of magnetic field topologies and field strengths, the field is controlled by plasma dynamics (convection and waves) from the bottom of the model up to some 1000 km above the photosphere (at $z = 0$ km) where plasma $\beta < 1$; the magnetic field dominates in the mid to upper chromosphere and in the corona above. In general we find that chromospheric temperatures (2000 K – 10 000 K) extend some 2 Mm above the photosphere, but the effects of non-linear waves and/or the magnetic topology can allow cool material to extend in extrusions several Mm higher. Photospheric and convective motions excite waves that propagate into the chromosphere. The compressive modes (acoustic waves and slow mode waves in the low-β upper chromosphere) rapidly become non-linear with height and dominate the dynamics and energetics of large parts of the chromosphere. At greater heights these waves are channeled by the magnetic field. The magnetic field, when strong, is also a direct source of heating, as current sheets dissipate in regions of large magnetic gradients. Thus, we find higher chromospheric temperatures near regions of enhanced magnetic field strength.

How well does the emission from such model chromosphere reproduce observed emis-

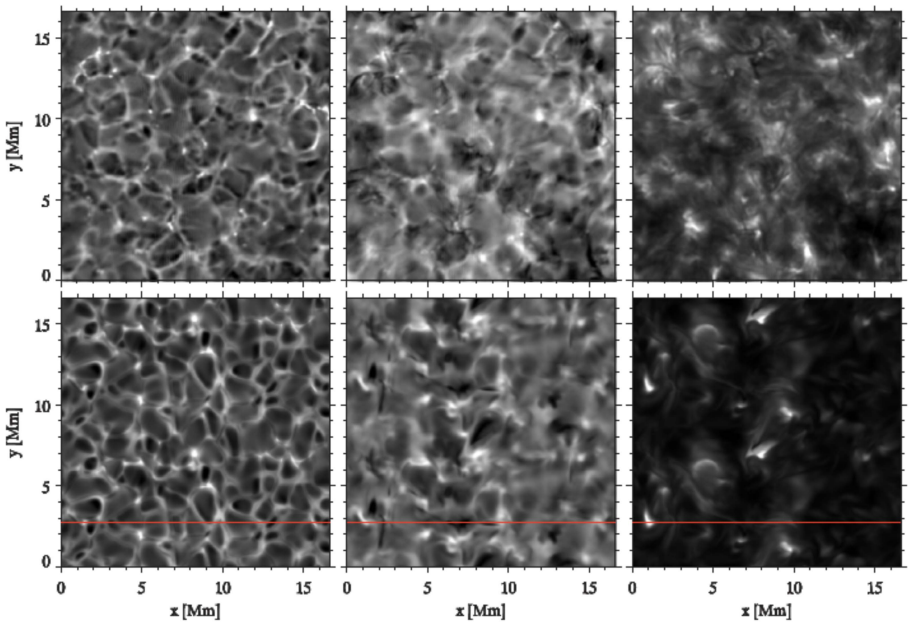

Figure 3: Observed (top panels) and synthetic (bottom panels) images of Ca II 854.2 nm at different postions in the line. Left in the line wing; middle in the "knee" of the line; right in the line core. From Leenaarts et al. [17].

sion statistically? In figure 3 we present one such comparison of the Ca II 854.2 nm line that is formed in the lower to mid chromosphere. In the line wings, representing plasma a few hundred kilometers above the photospere the synthetic and observational images are nearly indistinguishable. This is also the case for the images made at the "knee" of the line (the wavelength λ at which $dI_\lambda/d\lambda$ changes amplitude) formed some 500 km above the photosphere. On the other hand, the line core formed at roughly 1.3 Mm, shows significant differences between the observed and simulated images [17]. In addition, it is also found that the line core profile is narrower in the simulated spectra than in the observations indicating that the Sun shows more vigorous large scale dynamics and motions at smaller scales than are resolved in this particular simulation. This conclusion is in part vindicated by simulations run at higher ($\times 2$) resolution, which gives line widths of order those observed.

Satisfying as these results from the mid chromosphere are, comparisons made between diagnostics made at greater heights in the atmosphere such as the Mg II k line shown in Figure 1 show significant discrepancies between simulated and observed data. In particular we find that the simulations show narrower line profiles and too little emission on average, especially in regions where the magnetic field is strong. This discrepancy is likely due to a paucity of chromospheric heating in the models, perhaps due to the lack of enough magnetic flux at small scales. The too narrow line profiles could also be caused by the lack of small scale dynamics in the simulations highlighting the need for higher resolution runs to be made. On the other hand, non-equilibrium physics could also play an important role. It is well known that the rates of hydrogen ionization and recombination [4], as well as those of molecule

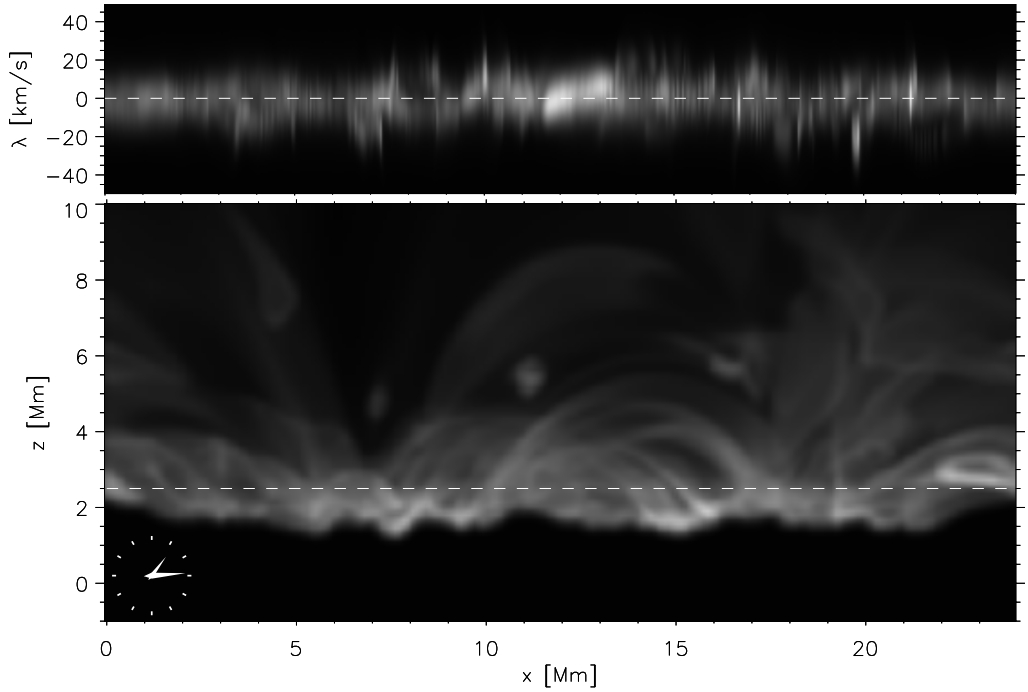

Figure 4: Synthetic observation of the Si IV 139.3 nm line as seen on the Solar limb. The top panel shows the line profile at the location of the dashed white line in the lower panel, which shows the total intensity of the Si IV line. The resolution of the synthetic images is degraded to that achieved by the IRIS satellite. From Hansteen et al. [11]

formation and disassociation [16], are quite slow compared to the dynamical timescales of the mid to upper chromosphere. Thus, the ionization state of the plasma should be carefully modeled; it can be important to include these processes in detail. In addition Martínez-Sykora et al. [19] stress the importance of the effects of partial ionization and generalized Ohm's law in the upper layers of the chromosphere which, amongst other effects, could give rise to differences in the current dissipation heating rate in the upper chromosphere.

Ascending still higher in the atmosphere, to the transition region, where the temperature rapidly rises from 10^4 K to 10^6 K, and to the corona where $T > 1$ MK we find an atmosphere mainly heated by the dissipation of currents generated by stresses in the magnetic field as it is braided by photospheric motions many pressure scale heights below. The heating generally follows the energy density of the magnetic field $\frac{B^2}{2\mu_0}$, but is also sensitive to the magnetic field topology.

The structure of the upper atmosphere is a result of the balance between the heating and the energy loss mechanisms available to the plasma: at high density and relatively low temperature ($< 10^5$ K or so) optically or effectively thin radiative losses dominate, while at lower densities and higher temperatures it is thermal conduction that controls the temperature structure. A consequence of this state of affairs predicted by the numerical models is

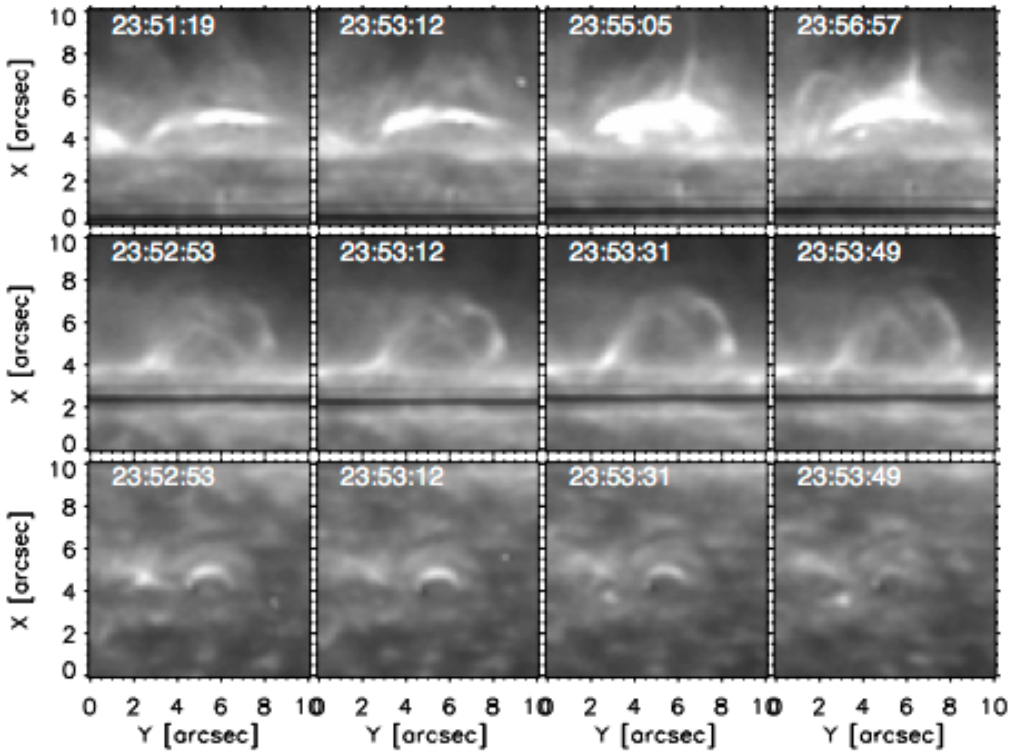

Figure 5: Three detailed views of UFS loops (see text) as observed with the IRIS satellite. These slit jaw images are images are taken in the Si IV band centered on 140 nm and representative of plasma at roughly 80 000 K.

the existence of low lying "cool" transition region loops [10, 11] with no thermal connection to the hotter coronal plasma, examples of which are shown in Figure 4. Observations made with IRIS show that such loops, visible in the Si IV band centered around 140.0 nm as seen in Figure 5, indeed form an important component in transition region emission [11].

To summarize, many characteristics of simulated emissivities in transition region lines such as C II 133.4 nm and Si IV 139.3 nm formed in the transition region and Fe XII 19.5 nm formed in the corona are similar to those observed [12]. On the other hand, phenomena such as spicules of type II are nearly absent [see e.g. 23, 5] indicating that the correct magnetic topology of the atmosphere has not been found, that the spatial resolution of the simulation is not sufficient, or that some important physical effects are still missing.

5 Conclusions

The IRIS satellite has opened up a new window into the solar chromosphere and transition region. These are regions that previously have been unexplored at high resolution, both due to the technological challenge of observing at the relevant wavelengths and due to the inherently complicated relationship between the observables and the underlying physical state of the atmosphere. With the advent of new computers and computational techniques several of these difficulties are solved. The models presented here show that simulations of the lower chromosphere seem to do well when compared with observations, though also that retaining sufficient spatial resolution to describe atmospheric dynamics is vital. Further, simulations predict that magnetic heating dominates in regions where $\beta < 1$, *i.e.* in the upper chromosphere (above 1 Mm) and in the corona. However, current models are not capable of reproducing the full wealth of IRIS observables, especially in magnetically dominated regions: The magnetic field needed to describe the upper atmosphere is observationally not well constrained. It also seems likely that numerical simulations must be run at higher spatial resolution.

In addition, it is also puzzling that a number of highly dynamic events such as spicules of type II prevalent in all IRIS observations of the limb are not reproduced in the numerical simulations. These differences between observations and models have the potential to teach us much about the Sun's upper atmosphere in the years to come.

Acknowledgments

This research is supported by the Research Council of Norway and by the European Research Council under the European Union's Seventh Framework Programme (FP7/2007-2013) / ERC Grant agreement Nr. 291058.

References

[1] Alfvén, H. 1947, MNRAS, 107, 211

[2] Beeck, B., Collet, R., Steffen, M., et al. 2012, A&A, 539, A121

[3] Carlsson, M. & Leenaarts, J. 2012, A&A, 539, A39

[4] Carlsson, M. & Stein, R. F. 2002, ApJ, 572, 626

[5] De Pontieu, B., Rouppe van der Voort, L., McIntosh, S. W., et al. 2014, Science, 346, D315

[6] De Pontieu, B., Title, A. M., Lemen, J. R., et al. 2014, Sol. Phys., 289, 2733

[7] Galsgaard, K. & Nordlund, Å. 1996, J. Geophys. Res., 101, 13445

[8] Gudiksen, B. V., Carlsson, M., Hansteen, V. H., & et al. 2011, A&A, 531, A154

[9] Gudiksen, B. V. & Nordlund, Å. 2005, ApJ, 618, 1020

[10] Guerreiro, N., Hansteen, V., & De Pontieu, B. 2013, ApJ, 769, 47

[11] Hansteen, V., De Pontieu, B., Carlsson, M., et al. 2014, Science, 346, 315

[12] Hansteen, V. H., Hara, H., De Pontieu, B., & Carlsson, M. 2010, ApJ, 718, 1070

[13] Hayek, W., Asplund, M., Carlsson, M., et al. 2010, A&A, 517, A49

[14] Hendrix, D. L. & van Hoven, G. 1996, ApJ, 467, 887

[15] Klimchuk, J. A. 2006, Sol. Phys., 234, 41

[16] Leenaarts, J., Carlsson, M., Hansteen, V., & Gudiksen, B. V. 2011, A&A, 530, A124

[17] Leenaarts, J., Carlsson, M., Hansteen, V., & Rouppe van der Voort, L. 2009, ApJL, 694, L128

[18] Mariska, J. T. 1992, The solar transition region, ed. J. T. Mariska

[19] Martínez-Sykora, J., De Pontieu, B., & Hansteen, V. 2012, ApJ, 753, 161

[20] Nordlund, Å., Stein, R. F., & Asplund, M. 2009, Living Reviews in Solar Physics, 6, 2

[21] Parker, E. N. 1988, ApJ, 330, 474

[22] Pereira, T. M. D., Asplund, M., Collet, R., et al. 2013, A&A, 554, A118

[23] Pereira, T. M. D., De Pontieu, B., Carlsson, M., et al. 2014, ApJL, 792, L15

[24] Skartlien, R. 2000, ApJ, 536, 465